

Modeling of vibratory pile driving

F. Rausche

GRL Engineers, Inc., Cleveland, Ohio, USA

ABSTRACT: Vibratory installation of piles and casings can be extremely economical and therefore the contractors' preferred method of pile driving. Compared to impact pile driving it also has the advantage of reduced noise pollution. Unfortunately, this installation method is still fraught with uncertainties. The foremost question is driveability and equally important is the question of bearing capacity of the installed pile. Both are difficult to answer prior to actually driving a pile. In other words, given a soil profile and pile type, the question of which vibratory hammer could drive the pile to a certain depth often cannot be answered with sufficient certainty. Once the pile has been installed, its bearing capacity cannot be calculated with sufficient accuracy based on the observed final rate of penetration.

Many attempts have been made to calculate the pile capacity based on the driving resistance, however, to date it is still required that the pile is redriven with an impact hammer for acceptance as a bearing pile. As far as driveability is concerned, simple charts issued by hammer manufacturers based on pile size or weight seem to be as reliable as other more sophisticated methods of hammer selection.

This paper summarizes current analytical methods and explains how wave equation analysis can be used in a manner comparable to the analysis of impact driven piles. Hammer and soil modeling details are discussed. A few examples demonstrate capabilities and limitations of the methods and, for the wave equation approach, sensitivity of results to important soil resistance parameters.

1 INTRODUCTION

The history of vibratory pile driving has been discussed by several authors among them Smart (1969), Leonards et al. (1995) and, Viking (2002). The latter dissertation is very much up to date and little can be added to its literature review. Viking reports that the first studies on vibratory pile drivers were done in Germany in 1930 and in Russia in 1931. The first production units were built in Russia during or after the Second World War. Their utility was quickly recognized, leading to new developments in France, Germany and the United States. Among the newer developments was the Bodine hammer, which produced frequencies in excess of 100 Hz. Called the Resonant Pile Driver, this machine achieved much higher penetration rates than those with "normal" frequencies at or below 20 Hz. Although resonance is a function of the mass of the driver and the size of the pile, it is probably reasonable to draw the dividing line between resonant and low frequency pile drivers at 50 Hz.

The analytical treatment of vibratory pile drivers has either been done with simple energy formulas or with discrete representations of pile and/or soil. Discrete models include integration, much as introduced by Holeyman, et al. (1996), or so-called wave equation analyses, e.g., GRLWEAP (GRL, 1998). Additionally finite element analyses have been tried (Leonard, et al. 1995) as an improvement over other methods.

2 OBJECTIVES OF VIBRATORY HAMMER MODELING

Vibratory installation of preformed piles and casings has an important economic impact. Installation times, only 10% of those achieved with impact hammers, are not uncommon. On the other hand, unexpected refusal may occur where impact hammers still drive efficiently. Also the vibratory ham-

mer may produce undesirable vibrations in nearby structures, a limitation that will not be discussed in this paper.

The economic advantage of the vibratory hammer can only be realized if the contractor correctly predicts which size hammer will drive the pile to a required depth. Additional savings would be realized if it were assured that the pile had the required bearing capacity after installation. The simulation of the installation by vibratory hammers should therefore enable the analyst to predict the rate of penetration vs. depth (driveability analysis). In addition, a so-called bearing graph should be constructed, which would relate the pile bearing capacity to the rate of penetration at the end of the installation. Examples of these relationships will be demonstrated below.

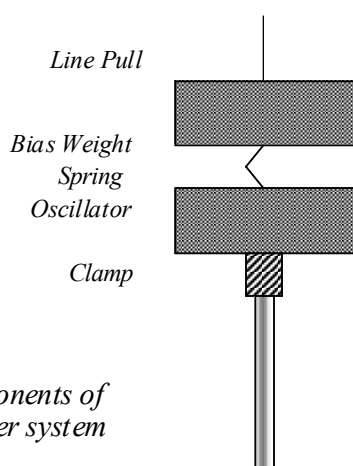


Figure 1: Components of vibratory hammer system

3 BASIC COMPONENTS OF A VIBRATORY HAMMER

The vibratory hammer, in its most common form, consists of pairs of eccentrically mounted masses which are contained in a frame whose appreciable mass may be called the oscillator. A bias mass isolates the oscillator from the hammer support – usually a crane line. The oscillator is separated from the bias mass by a very soft spring (Figure 1). The bias mass therefore adds a static force to oscillator and pile. The force in the crane line reduces this static force and, if it is greater than all weights, allows for pile extraction. Conveniently, the pile is attached to the oscillator by means of a hydraulic clamp. This connection may be considered rigid and, for modeling purposes, the clamp can be considered an integral part of the oscillator mass.

When eccentrically supported masses (combined eccentric mass m_e) spin at a rotational frequency $T = 2B f$ (f in Hz), their centrifugal force is

$$F_c = m_e T^2 \quad (1)$$

This centrifugal force (actually it differs slightly from Eq. 1 because of the oscillator's vertical motion) is transmitted through the eccentric mass bearings to the oscillator and thus to the pile. Only vertical components of the centrifugal force are transmitted to the pile because pairs of eccenters are spinning in opposite directions. Normally the hammer frequency is between 20 and 40 Hz and each peak compressive force generated by the vibratory hammer therefore occurs at intervals of 25 to 50 ms. For a resonant hammer, successive peak force values may occur at intervals of only 8 or 10 ms.

The free-free frequency, f_f , of a 20 m steel pile of wave speed $c = 5120$ m/s is

$$f_f = c/2L = 5120/40 = 128 \text{ Hz}$$

Comparing this free pile frequency with that of a low frequency hammer shows that resonance is unlikely in piles of normally encountered lengths. However, the mass of the vibratory hammer and the clamp, attached through the clamp to the pile, tends to reduce the lowest frequency of the overall system and, when piles get long and drivers heavy, makes resonance possible. According Poulos et al. (1980) the lowest resonance frequency of a system roughly reduces to 50% of the pile frequency if the mass on top of the pile equals the weight of the pile.

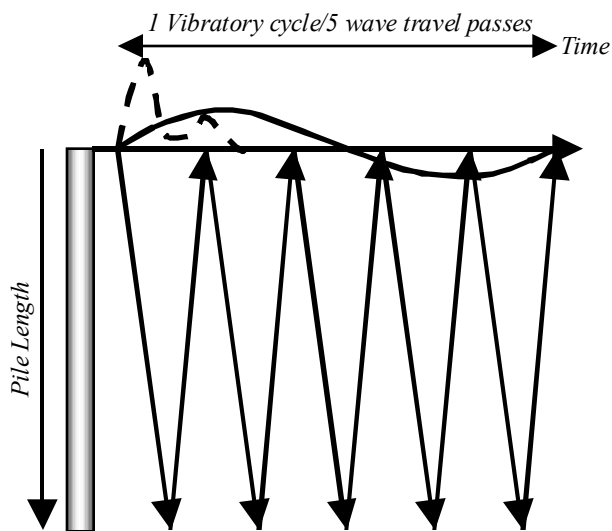


Figure 2: Comparing typical impact and vibratory hammer records

If the hammer frequency is significantly lower than the hammer-pile frequency, then the particles of the pile have practically the same direction of motion at the same instance in time. Figure 2 demonstrates in a length-time diagram the different loading patterns of a vibratory hammer and an impact hammer. The relationship shown is approximately scaled

for a steel pile of 20 m length and a vibratory hammer with a 25 Hz frequency.

Because of the relatively slow upward and downward motion of the pile under a vibratory hammer, many mathematical models ignore the elasticity of the pile and treat the pile as a single mass, acted upon by the oscillator force. The soil may then be considered an ideally plastic material, which reacts with an upward directed force during the downward pile motion and in downward direction when the pile is pulled upwards.

4 RESONANCE EFFECTS

It is important to distinguish two resonance effects:

- (1) Resonance in the soil has been observed to occur at relatively low frequencies (e.g. around 10 Hz) therefore occurs primarily during hammer start-up and shut-down, unless the hammer is equipped with a variable eccentric moment that can be reduced before the frequency is varied through the resonance range. This effect has been discussed in detail by Massarsch (1992). Only those models that include the mass and stiffness properties of the soil surrounding the pile have a chance of correctly predicting the soil resonance phenomenon.
- (2) Resonance in the hammer/pile system may occur at several frequencies. As discussed earlier, a low frequency resonance is possible depending on the relative magnitude of the hammer and pile masses. Resonance will also occur near the piles basic frequencies. Only those pile models that represent it's flexibility have a chance of correctly predicting hammer/pile resonance.

5 REFUSAL CRITERION

Refusal is defined as a certain limiting rate of penetration (mm/s). Smart defines it as 6.2 mm/s. Viking suggests 8 mm/s, citing the danger of excessive heat development in sheet pile locks. Of course, where bearing piles are driven, the lock friction is not of concern. In that case the pile could be driven to lower rates of penetration. For example, impact hammers typically are used to sets as low as 1 mm per blow with blow rates around 1 blow/s. Thus, from a productivity point of view, 1 mm/s still appears to be an acceptable rate of penetration.

Rate of penetration is not necessarily the only criterion for refusal conditions. Stresses in the pile, particularly around the clamp also must be considered. A realistic pile model can be particularly helpful for hammer and pile selection if the hammer is capable of predicting accurate stress levels near hammer/pile resonance.

6 SIMPLIFIED APPROACHES AND ENERGY MODELS

Consider the basic energy formula used for impact driven piles

$$R_u = 0E / (s + s_L) \quad (3)$$

Where R_u is the ultimate pile capacity; 0 is an efficiency, which reduces the theoretical hammer energy, E , to its actual value; s is the set per blow and s_L is a displacement value covering losses in pile and soil. Adding to the reduced hammer energy the energy that the system's weight, W , (hammer and clamp minus crane line pull) adds, one obtains

$$R_u = (0E + Ws) / (s + s_L).$$

Dividing the numerator and denominator of this equation by the time for one complete cycle $T = 1/f$, then this formula becomes

$$R_u = (P + W v_R) / (v_R + f s_L) \quad (4)$$

Table 1a: Pile properties after Smart (1969)

Pile	Type	Length (est.) m	Area cm ²	Penetr. (est.) m	Hammer Power kW	Hammer Frequency 1/s	Soil
62,1	HP14x117	30	221	27	343	107	Silt; dense to very dense Sand
62,2	HP14x117	30	221	27	310	113	Silt; dense to very dense Sand
62,3	HP14x117	30	221	27	343	107	Silt; dense to very dense Sand
78, 1	HP14x117	30	221	18	343	91	Cemented Sand; Clay
83, 1	CE-Pipe	24	47-54	20	37	43	Sand: N=31 to 61
83, 2	CE-Pipe	24	48	20	37	49	Sand: N=31 to 61

where P is the power actually supplied by the vibratory hammer's power unit (for that reason an efficiency factor is not needed), v_R is the rate of penetration (averaged over one cycle) and s_L is a loss term, to be determined empirically as in a pile driving formula. This is the Davisson formula according to Smart (1969). Recommended values for s_L range between 0.001 and 0.1 and may average 0.03. Also, according to Smart, Bernhard performed model pile studies and modified the power formula as follows:

$$R_u = (8P / v_R)(L/D) \quad (5)$$

The loss factor 8 not only covers power losses, it is an empirical adjustment factor and is to be set to 0.1 unless other correlation data exists. The L/D (pile length divided by pile penetration) may have an effect when the pile is only partially driven.

Davisson's power formula was modified and tested by Smart on more than 60 cases where rate of penetration and power readings were available. In several cases for which load test information was also available, Smart developed load-set curve dependent adjustment factors in a so-called "permanent-set method". This method is not further discussed here as it adds undue complexity to what should be a simple formula.

The case studies demonstrated by Smart represented primarily piles installed with a Bodine Resonant hammer with frequencies between 43 and 144 Hz and system weight $W=98\text{kN}$. Results from Equation 4 and 5 are demonstrated in Table 1b for 5 of Smart's load test cases, described in Table 1a.

Table 1b: Results from Power Formulas

Pile	Rate of Penetr. mm/s	Load Test kN	Davisson			Bernhard kN
			0.1 kN	0.03 kN	0.001 kN	
62,1	132.1	2314	882	1667	2642	289
62,2	8.9	2492	1049	3268	26399	3869
62,3	15.2	3560	1201	3561	19192	2502
78,1	4.6	2270	1458	4649	49918	12509
83,1	91.4	490	230	372	500	51
83,2	67.6	668	229	419	638	69

These results show that Bernhard's formula yields rather unreliable results with minima and maxima between 10% and 550% of the load test result. Davisson's formula varies between 34 and 2200% if the full recommended range of adjustment factors is considered. The medium factor of $s_L = 0.03$ inch/s produces a scatter between 63 and 205%. This relatively good result may be attributable, at least in part, to the fact that this same data was included in the study that led to the recommended loss factors. For other sites and hammers, different loss factors may be needed.

The simple power balance equations suffer from a very important defect: they do not consider the relative magnitudes of end bearing and shaft resistance, which, as we shall see affect driveability and bearing capacity evaluations to a significant degree. Furthermore, power formulas do not consider the type of soil into which the piles are driven.

Most disturbing, however, for all potential capacity determination methods is in Smart's data the apparent fact that the rate of penetration is unrelated to bearing capacity; for illustration, Figure 3 depicts load test capacity vs. penetration rate for the four H-piles of Tables 1a and 1b. Note that soil types were similar and that power and frequency varied only slightly for these four cases.

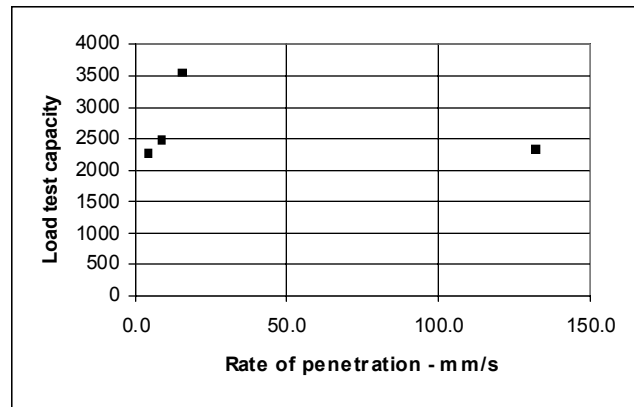


Figure 3: load test capacity vs. rate of penetration for the four piles of Table 1

7 CASE METHOD

The Case method was developed in the 1960s for impact driven piles on which measurements of force, $F(t)$, and velocity, $v(t)$, are taken near the top of the pile during driving. The Case Method formula for the evaluation of the instantaneous static resistance force, $R(t)$, was derived assuming an elastic pile and a soil resistance that acts in one direction (upward when the pile moves downward). The Case Method formula then becomes (Rausche et al., 1985)

$$R(t) = \frac{1}{2} (F_1 + Zv_1)(1 - J_c) + \frac{1}{2} (F_2 - Zv_2)(1 + J_c) \quad (6)$$

Where F_1 is the measured force at time t

F_2 is the force at time $t + 2L/c$

v_1 is the velocity at time t

v_2 is the velocity at time $t + 2L/c$

$Z = EA/c$ is the pile impedance

J_c is a dimensionless damping factor

L is the pile length

c is the wave speed in the pile material

E is Young's modulus of the pile material

A is the cross sectional area of the pile material.

For a rigid body the time $2L/c$ reduces to zero and thus $F_1 = F_2 = F(t)$ and $v_1 = v_2 = v(t)$ and the formula becomes

$$R(t) = F(t) + M a(t) - J_v v(t). \quad (7)$$

Eq. 7 is adequate for low frequency hammers. For higher frequencies, near the hammer-pile system's resonance level, the Case Method equation for elastic piles (6) would be more reasonable. Formula (6) approaches (7) as the pile length approaches zero and the pile becomes a rigid body of mass, M , with acceleration $a(t)$. The damping factor, J_v , is equivalent to the product of $Z J_c$.

7.1 Example – Case Method applied to an offshore pile

For low frequency hammers, Eq. 7 is satisfactory as shown by Likins et al. (1992) who described how a 1520 mm diameter pipe of 40 m length was driven with an ICE 1412 hammer (115 kg m, 21 Hz, 410 kW) through 13.4 m of sand into a firm to very stiff clay. The pile met refusal at a depth of 19.2 m and was then driven with a Vulcan 060 steam hammer starting at a blow count of 75 blows per 0.3 m of penetration. A reasonably accurate correlation was obtained between the positive peak value calculated by the rigid body Case Method formula and a dynamic impact test following the vibratory installation. In this case J_v was set to zero. (The lack of damping reduction may have been offset by the soil setup occurring between end of vibratory driving and the beginning of the impact test.) Figure 4 depicts a portion of the record taken at the end of the vibratory driving together with related, calculated pile variables. The force and acceleration records were evaluated according to Eq. 7 and indicated 2820 kN peak soil resistance while the impact records yielded a CAPWAP capacity of 3050 kN.

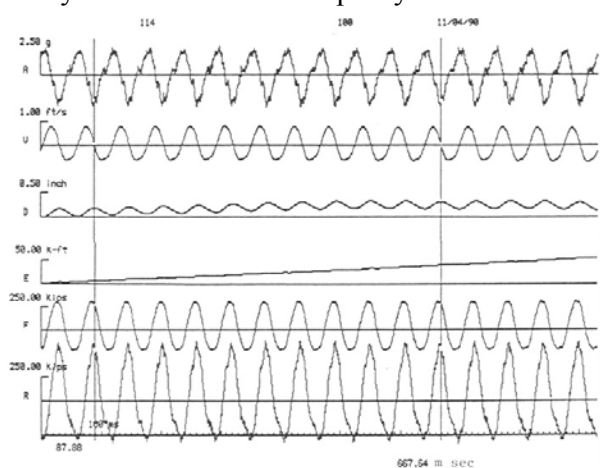


Figure 4: Measurement results from offshore pile, from top: acceleration, velocity, displacement, transferred energy, force and resistance after Eq. 7.

8 INTEGRATION METHODS

The name “Integration Methods” was used in Viking (2002) for an approach which (a) formulates a force balance for a rigid pile, (b) uses Newton’s Second Law to calculate acceleration and (c) integrates the acceleration to obtain the rate of pile penetration. Viking uses this name for rigid body models of the pile and either concentrated or discretized soil models such as the model of Holeyman et al., 1996. Viking differentiates between pile integration methods having rigid pile models from wave equation type models even though the latter also integrate motions calculated from a force balance. The difference is that the process is repeated for the segments of a discretized elastic pile.

The basic model of Holeyman et al. (1996) is depicted in Figure 5; it not only includes the shaft resistance and end bearing but also lock friction. Actually, shaft resistance and lock friction are treated in

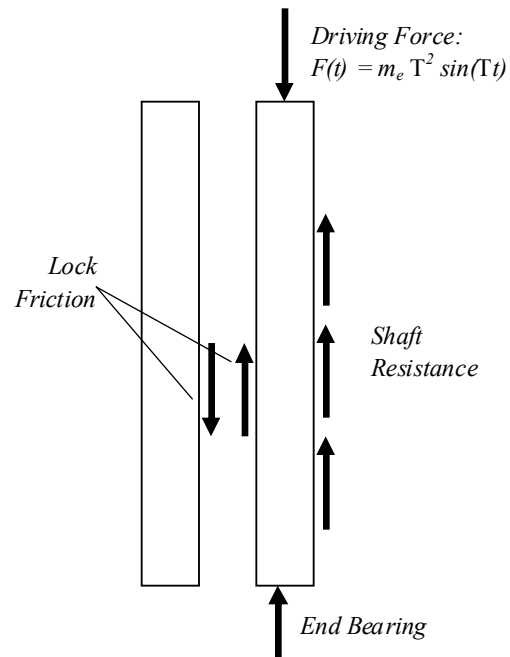


Figure 5: Sheet Pile model after Holeyman et al. 1996.

the same manner, i.e. as ideally plastic resistance components. More importantly, the shaft resistance is distinguished from end bearing by allowing it to have a negative downward resistance during the upward pile motion while end bearing only has a positive component. Holeyman’s simplified model calculates the velocities during the upward and downward motions. The resistance components are modeled as ideal plastic forces acting at shaft and toe. An important part of Holeyman’s model is the reduction of the static shaft and toe resistance to so-called liquefied values. The algorithm requires an iterative analysis of soil and pile resistance since the liquefaction of the soil is considered a function of the vibration amplitude.

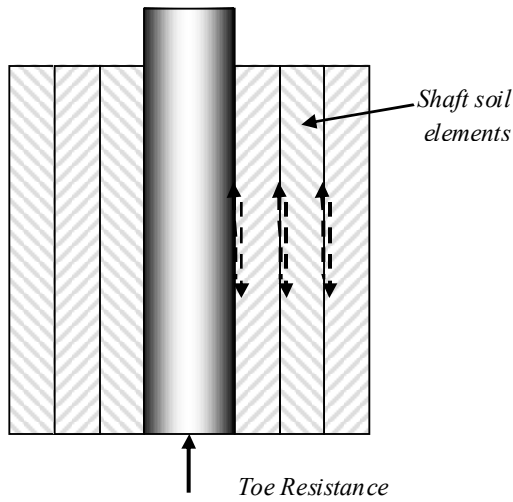


Figure 6: Vipere pile and soil model, after Viking 2002

Viking describes also the more elaborate Vipere soil model after Vanden Berghe (Figure 6). It includes a hyperbolically behaving shaft resistance and a practically bilinear toe resistance. The Vipere shaft resistance calculation is based on the analysis of several cylindrical soil elements, as proposed by Holeyman et al.(1994), surrounding the pile to model radiation damping associated with the shaft resistance. A degradation algorithm of the shaft resistance as a function of soil strain is also included in this model. The shaft resistance model appears to be symmetric, i.e. the upwards directed resistance forces and the downwards directed resistance forces have equal magnitude. The Vipere soil model parameters are based on laboratory test results.

The Vipere toe model is shown in Figure 7. It is interesting to compare this model with the wave equation toe model discussed below and depicted in Figure 8c. Both models move with zero resistance through the “gap” created in the previous cycle. However, the Vipere toe model has a bilinear behav-

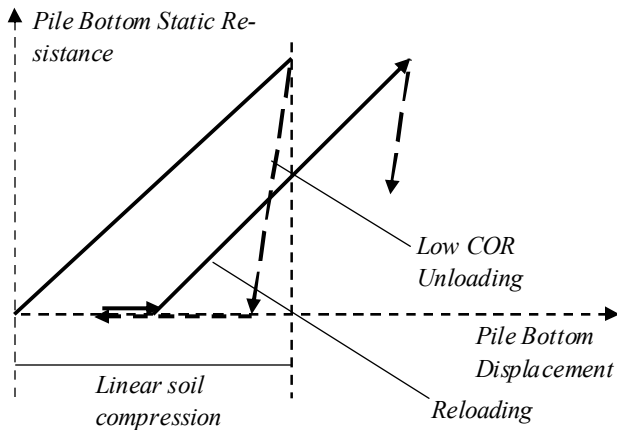


Figure 7: Vanden Berghe toe resistance model after Viking 2002

ior with a practically infinite stiffness during unloading (coefficient of restitution, COR, near zero), thereby dissipating all energy stored in the soil spring. The wave equation model, on the other hand, consumes energy only after plastification and through the associated viscous damping model.

8.1 Modifications to the wave equation approach

Although the rigid pile model seems to be satisfactory as long as the piles are of moderate length and the hammers of “normal” low frequency, efforts have also been made to adapt the wave equation approach to represent the vibratory hammer, pile and soil. This is reasonable for a number of reasons. First, existing computer programs offer a detailed procedure easily used by the analyst. Second, although pile elasticity is not a crucial parameter for analyzing low frequency hammers, the wave equation approach offers a rational means of analysis over a wide range of hammer frequencies and a simple approach to representing soil resistance forces. Since increasingly heavier hammers and larger piles are used, resonance effects may be more and more frequent and would go unrecognized by the rigid pile analysis. Additionally, the wave equation analysis

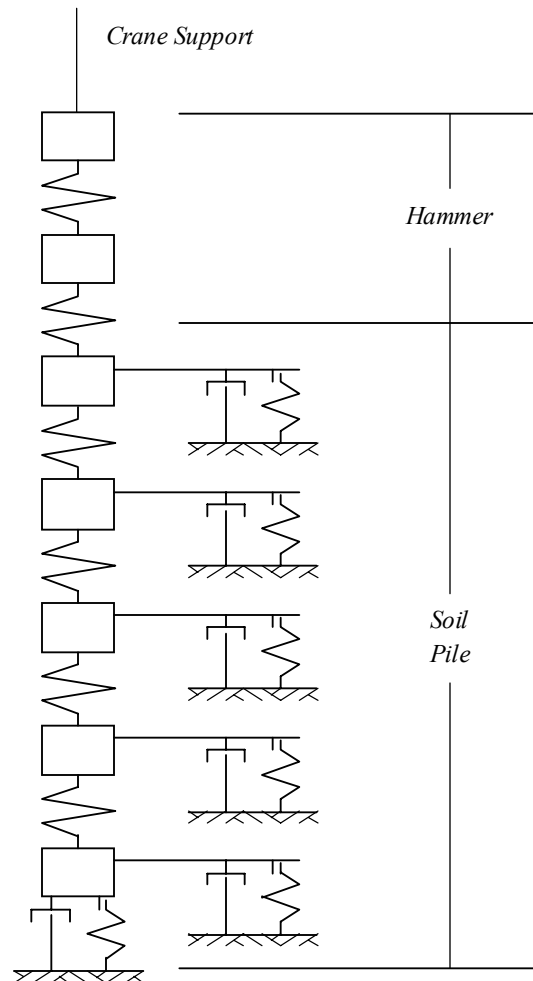


Figure 8a: The wave equation model

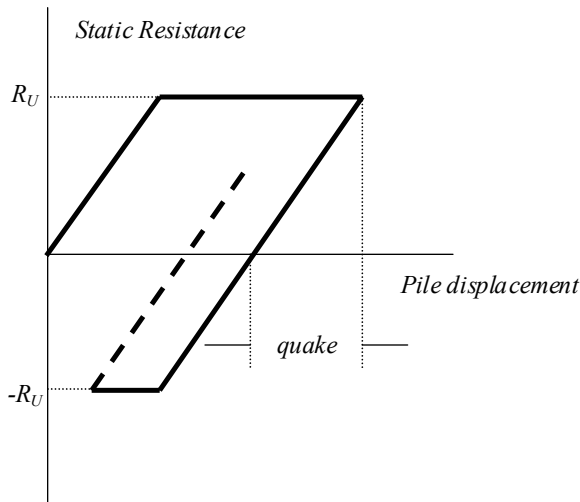


Figure 8b: Smith static shaft resistance

readily calculates stresses in the pile, which may be important when resonance is imminent. Most importantly, the wave equation concept has been adopted by many practitioners around the world; to the practitioners it would be most convenient if the same approach could be used for vibratory analysis as for impact hammer analysis.

The wave equation model according to Smith(1960) (Figure 8a) has been described in detail in papers and manuals (e.g. GRL 1998). Its soil model includes an elasto-plastic static resistance with parameters quake and ultimate capacity. The static resistance on the shaft (Figure 8b) is assumed to be symmetric, i.e. it has during upward motions the same magnitude of resistance as during downward pile motions but with opposite sign. Thus over one cycle, the impulse of this shaft resistance is zero. The toe model is similar, yet it has no negative resistance components (Figure 8c). The Smith soil resis-

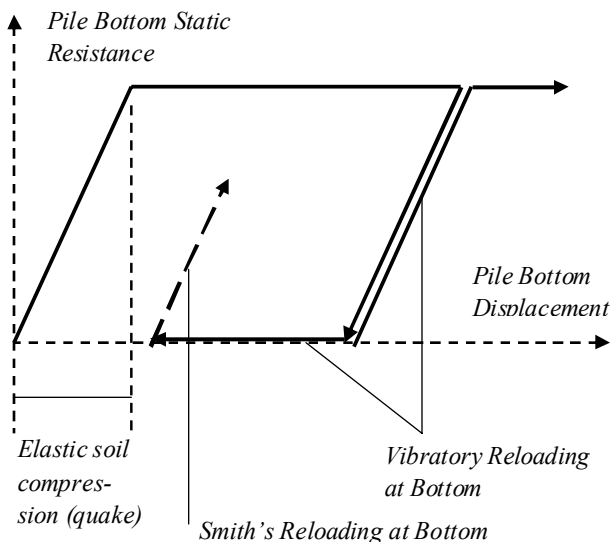


Figure 8c: Vibratory toe model in GRLWEAP

tance model also includes damping at shaft and toe, calculated as the product of damping parameter, static resistance and pile velocity.

Modifications necessary to produce reasonable results for vibratory pile driving simulations by GRLWEAP include the following.

1. The hammer model has to accommodate the sinusoidal forcing function over a relatively long time period. For example, a typical impact event is finished within 50 ms. In contrast, it may be necessary to analyze the vibratory motion for up to 2000 ms until a convergence in the pile variables is achieved. A long duration analysis is particularly important when analyzing a hammer with very low frequency.

2. During the analysis residual forces build up in pile and soil. These residual forces are essential for the driveability evaluation and therefore must be accurately included in the analysis. The analysis can only be stopped after the residual stresses, and therefore the pile motion, converge within a certain criterion. The residual stresses only occur where shaft resistance forces exist which exert a downward force on the pile when either the hammer applies an upward force or the pile rebounds.

3. The model must calculate power consumed by the hammer and if this value exceeds the rated value, reduction of power output must be automatically accomplished.

4. The model must include the force of the crane line and allow for extraction if this force exceeds the weight of the system. Similarly, it should be possible to analyze the pile penetration under a crowd force.

5. Instead of blow count and set per blow, the program has to calculate the rate of penetration or the time per unit penetration.

6. The end bearing has to be much more carefully modeled than for impact driving because of the separation of the pile bottom from the soil during the upward motion. Figure 8c compares the standard static toe soil resistance model according to Smith with a model that has been found to be most reasonable for vibratory analyses. In this modified static end bearing model the pile bottom will move through the gap generated in the previous cycle with zero resistance until the point of maximum displacement minus elastic rebound is reached. If the standard model were

used, the pile will work itself out of the ground unless it has a large shaft resistance. This model may be called “Residual Toe Gap”. The traditional model could be referred to as a “Closing Gap”. It is conceivable that the Closing Gap analysis is more reasonable than the Residual Gap model under soil conditions, such as soft clays or loose submerged sands, particularly when frequencies are low. Fortunately, the soft or loose strata do not cause high end bearing values and therefore introduce little uncertainty.

7. Energy losses are modeled with (a) Coulomb damping of the elasto-plastic static soil resistance component and (b) viscous damping. Since the particle velocities are usually lower than for impact driven piles and since the damping behavior is non-linear (Coyle et al., 1970) it is suggested to use Smith-viscous damping with damping factors, J_{SV} , which are double the normally suggested Smith damping factors for impact driven piles. Thus,

$$R_d = R_U v J_{SV}$$

where R_U is the ultimate soil resistance at a segment, v is the pile velocity, and J_{SV} is the Smith-viscous damping factor.

Table 2: Results from sensitivity study

Case	Q shaft	Q toe	Jshaft	J toe	Toe	Refusal
	mm	mm	s/m	s/m	Cap.	Capacity
1	5	5	1.3	1	235	780
2			2	1.5	180	600
3			0.65	0.5	270	900
4	2.5	2.5	1.3	1	338	1125
5	5	5	1.3	1	90	860
6					270	540

8.2 Example, driveability with Vipere and wave equation

This example was taken from Viking (2002) and describes the driving of a sheet pile (cross sectional area 95 cm^2 and length 14m) with an ABI hammer (MRZV 800V). This unit has a variable eccentric moment with a maximum of 12 kg m and was run at 41 Hz. Below a 2.5 m thick clay layer, the soils consisted of silty sand and sand to the installation depth

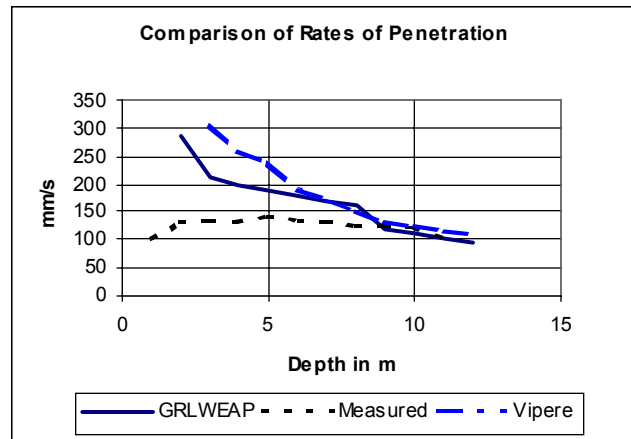


Figure 9: Calculated and measured penetration rates after Viking (2002)

of 12 m where the cone resistance varied between 2 and 4 MPa.

The wave equation analysis was run with typical quake values of 2.5 mm and double Smith-viscous damping values were chosen as follows: 0.33 s/m in the sand, 0.60 s/m in the silty sand and 1.2 s/m in the clay. For the toe, the damping was set to 1.0 s/m. For the sand it was assumed that the unit shaft resistance increased from 10 to 15 kPa and that the toe resistance increased from 10 to 15 kN. The driveability analysis results of the Vipere and GRLWEAP analyses are shown in Figure 9. Obviously, the calculated rates of penetration were well predicted for the 12 m depth but were grossly over predicted for the early part of the analysis by either analysis. Viking suggested that lateral motions in the early driving portion caused a reduced rate of penetration.

8.3 Example, sheet pile driving

A double sheet pile section was driven with an ICE 815 vibratory hammer as part of a cellular cofferdam installation. This hammer has an eccentric moment of 51 kg m and was run at 22.5 Hz. In order to avoid problems with misalignments, the contractor drove sheets short distances, working successively around the circular cofferdam. The soil was cohesive and relatively early refusal was the reason why measurements were taken during vibratory driving. It was concluded the soil setup along with lock friction caused the problems.

The analysis was done with a 0.7 efficiency based on field measurements of force and velocity. The calculated bearing graph is shown in Figure 10; it used double the normal quakes and double damping factors. As can be seen, stresses and capacity calculated with these parameters agreed quite well with measurements.

This example is suitable for a check on the sensitivity of some of the soil parameters of the wave equation approach. Table 2 shows capacities that were calculated when varying damping values, quakes and the percentage of the end bearing. Obviously, refusal capacities are equally sensitive to all three quantities varied with the quake reduction from 5 to 2.5 mm allowing for the greatest increase in capacity. On the other hand, with damping and quake values the same, an increase of end bearing percentage from 30 to 50% had the most pronounced effect on capacity. Clearly, for a given set of soil parameters there is a limiting end bearing (in this case around 300 kN) that cannot be overcome by the system.

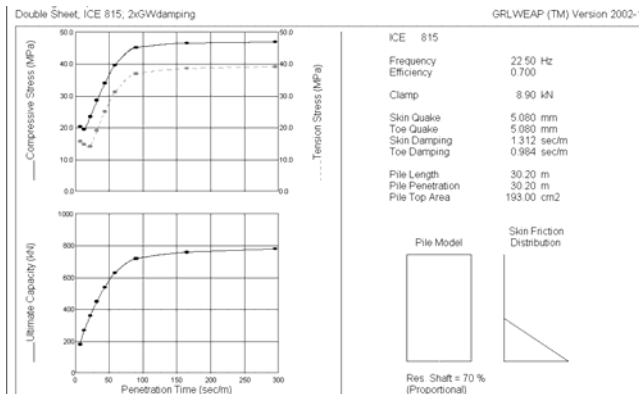


Figure 10: Results from GRLWEAP sheet pile analysis with double quakes and double damping and comparison with measured results for (from top) compressive and tensile stress and capacity at 1600 s/m rate of penetration.

8.4 Example, reanalysis of pipe pile data

ile 83,1 (Table 1) was one of the better documented cases in Smart (1969) and most data needed for an analysis by GRLWEAP was available. The hammer was a Bodine resonance pile driver run at a relatively low frequency of 41 Hz and with a reduced moment of 0.94 kg m. Using standard soil resistance parameters for the silty sand and sand strata, i.e. double damping factors and 2.5 mm quakes, refusal penetrations were calculated for capacities exceeding the static weight of the driving system. On the other hand, Smart's field observations suggested a final penetration rate of more than 90 mm/s and a load test capacity of 490 kips. The static weight of the system was approximately 110 kN. The calculated displacement vs. time graph, shown in Figure 11, gives one explanation for the disagreement: the calculated dynamic double-amplitudes at the pile top and toe were only 0.57 and 0.27 mm, respectively, and therefore much less than the quake values of 2.5 mm. (Note that the constant displacement offset is

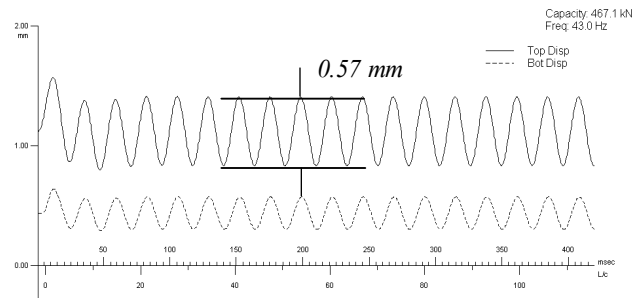


Figure 11: Calculated displacements of Pile 83,1 Table 1a

due to the elastic pile penetration under the static weights.) Since neither static nor dynamic forces were sufficient to fail the soil, it is not surprising that the analysis did not predict any appreciable pile penetration. This is the only example that clearly shows that the soil must have been in a reduced state of strength during driving, even though the power equations suggest that the pile bearing capacity during driving was close to that in the load test.

8.5 Example, resonance calculations

A special hammer was built and tested in the yard of the hammer manufacturer where weathered rock was encountered less than 4 m below surface. The surficial materials consisted of cohesionless soils. The hammer had an eccentric moment of 3.8 kg m and was designed for frequencies up to 80 Hz. A closed ended pipe of 170 mm diameter and 18 m length was instrumented with strain transducers and accelerometers and was rigidly bolted to the oscillator (12.4 kN weight). The bias weight was 29 kN.

One of the questions to be answered by the test was the behavior of this hammer in the neighborhood of resonance. Resonance for the pile alone on rock would occur at approximately 7 Hz ($c/4L$, i.e. wave speed in steel divided by 4 times the pile length); according to Poulos et al. (1980), for the above hammer weights, the resonance frequency of the hammer-pile system would be near 14 Hz.

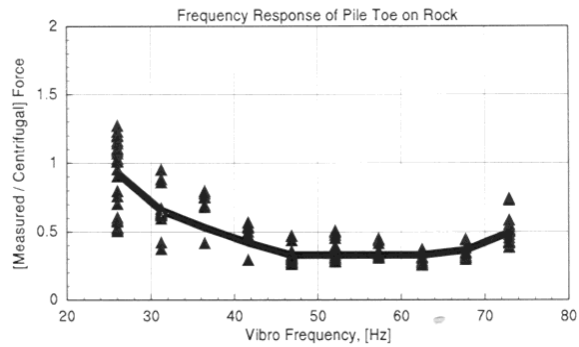
Resonance was checked by dividing the maximum measured pile top force by the centrifugal force. The available measured data (Figure 12a) indeed suggests that the force ratio increases near the 14 and 70 Hz hammer frequencies. Unfortunately, because of a limited power rating of hammer and power pack, unlimited resonance forces could not be measured.

A check was made on the pile behavior by GRLWEAP calculating pile forces, power dissipation in the pile and force ratio. These results are shown in Figures 12b and c and very clearly indicate the same tendency as the measurements. However, in order to avoid that the program automatically reduced the power output which would have made a

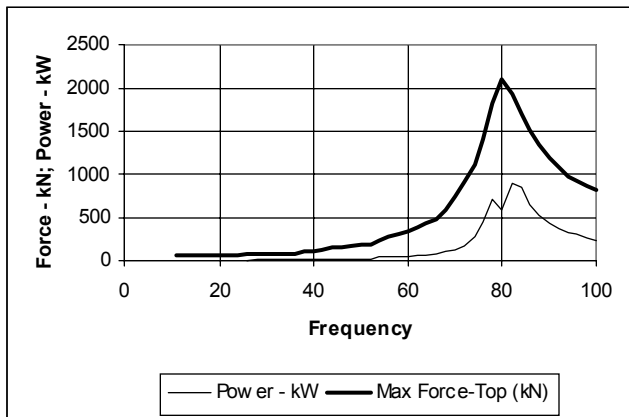
8.6 Example, large caisson

This example has been discussed by White (2002). It deals with a 12 m diameter by 0.25 m thickness concrete caisson of 25 m length. The caisson was tapered down to 0.21 m thickness at mid-length. Four APE 4B hammers with 683 kg m eccentric moment and 750 kW power each were employed with frequencies between 19.4 and 20.8 Hz. Soils consisted of clay, silty sand, sand and again silty sand with N-values of at most 3. For the analysis it was assumed that the unit shaft resistance and unit end bearing would be 10 kPa (degraded to 80% during driving) and 90 kPa, respectively. The total shaft resistance was figured for the inside and outside area of the cylinder. Damping was set to 1.3 and 1.0 s/m at shaft and toe and quakes were set to 2.5 mm. The observed final penetration times at 12 m depth ranged between 37 and 53 mm/s. The wave equation calculated penetration times are plotted vs. depth in Figure 13. They were 36 and 50 mm/s for 100% and 80% of the assumed static resistance values at the final penetration. Most of the penetration occurred prior to vibratory driving due to the static weight of hammers, transfer beams and caisson.

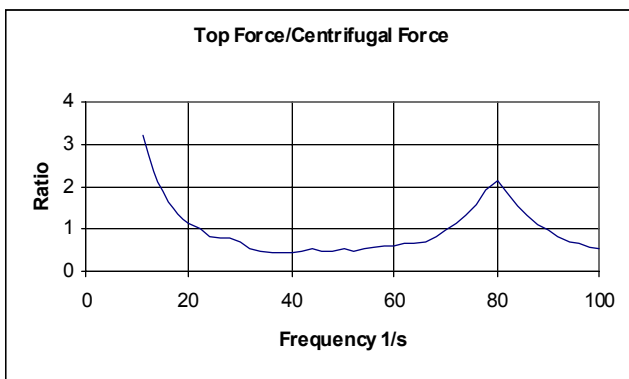
One of the advantages of analyzing an elastic pile model is the possibility of calculating reasonably accurate pile stresses. In the case of the concrete caisson, calculated stresses were at most 1.5 MPa. This stress is equivalent to a force of 13.8 MN. One quarter of this stress had to be transferred at each of the four points where the transfer beams were attached to the pile top.



(a)



(b)



(c)

Figure 12: a) measured force ratio b) GRLWEAP calculated forces and power transferred to top of pile; c) ratio of pile top force to centrifugal force;

resonance check difficult, the power rating was arbitrarily set to an unrealistic high value of 1000 kW. For that reason, calculated power transfer and forces at the pile top reached much higher values than during measurements. Still, the tendency is obvious: resonance is indicated in the 15 and 80 Hz range. In fact, during the test when the hammer frequency was increased to values above 70 Hz, the stresses in the pile became so high that the pile-oscillator connection ruptured. It should be pointed out that such relatively realistic resonance studies can only be successful with an elastic pile model.

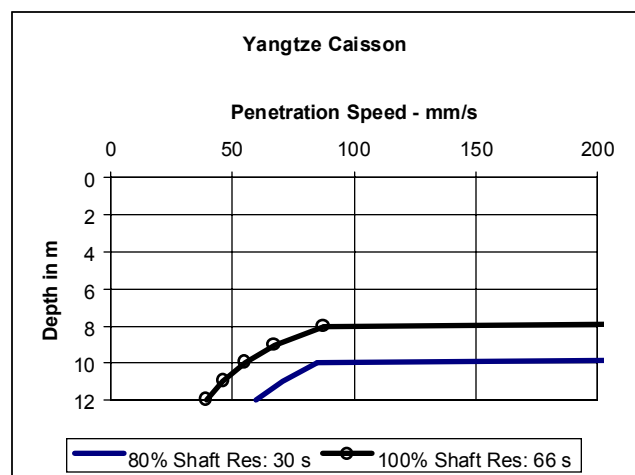


Figure 13: GRLWEAP drivability results for a large caisson

9. FINITE ELEMENT METHODS

For the sake of completeness it should be added that Leonards et al.(1995) reports, how FLAC (Fast Lagrangian Analysis of Continua), a finite element

code, was adapted to the analysis of vibratory pile driving. The researchers only modeled cohesionless soils in their study. For loose sands they considered a strain hardening model and for dense soils a strain softening model. Based on the calculated stress-strain history, both shear stress and void ratio would approach the steady state values. The transverse displacements, i.e. radiation damping, in the soil were tracked as a function of time. The computer program typically required several days for an analysis.

This initial study did not get into details about vibratory pile driving specific model details. It appears that it was limited in scope due to lack of funds. Preliminary results appeared to be reasonable, and it appears that this is an interesting research tool for future studies.

10. SUMMARY

The following conclusions can be drawn from the examples analyzed.

- Reliability of prediction of vibratory pile driving is still elusive. There are still many unanswered questions.
- The absolute magnitude of shaft resistance (or the shaft quake) is less important than the absolute magnitude of end bearing. If the percentage of shaft resistance is low then the pile can only be driven if the sum of crowd force and weight of all components exceeds the end bearing.
- The stiffness (quake) of the shaft resistance is as important as the absolute magnitude of the shaft resistance. It is possible that this parameter varies as much due to vibration as the soil resistance itself.
- The end bearing elastic properties have to be as carefully considered as the magnitude of the end bearing.
- Both static elastic and dynamic resistance parameters can have a decisive effect on drivability.
- In general, reasonable agreement between field observations and analysis can be achieved even without a liquefaction model for the shaft resistance.
- Stress predictions, even near resonance, can be made with reasonable accuracy.

11. RECOMMENDATIONS FOR ADDITIONAL WORK

The following studies and improvements should be made to aid the practitioner in the proper selection of vibratory piling equipment and for a better assessment of vibratory driven pile capacity.

- Most studies on vibratory pile driving deal with cohesionless soils. However, cohesive soil types pose more important questions regarding drivability than sands.
- Correlation studies dealing with the prediction of the bearing capacity of vibratory driven piles have to consider carefully the effects that the final cycles before hammer shut-off. For example, it may be necessary to require a certain procedure at the end of installation (e.g. certain final frequency while the eccentric moment is reduced to zero) to assure consistent capacity results.
- The differences between high frequency-low amplitude vibratory pile driving and lower frequency-high amplitude are still not understood and should be investigated.
- A method for calculating the increase or decrease of end bearing due to vibratory pile driving should be established for both cohesive and non-cohesive soils.
- Since liquefaction at the shaft does not seem to have a pronounced effect on drivability it is suggested to spend less effort on sophisticated resistance degradation models for the shaft and much greater efforts on investigating the change of pile toe resistance.

12. REFERENCES

- Coyle, H.M., and Gibson, G.C., 1970. Empirical damping constants for sands and clays. ASCE, Journal of the Soil Mechanics and Foundations Division.
- GRL, Goble Rausche Likins and Associates, Inc. 1998. GRLWEAP, wave equation analysis program, 4535 Renaissance Parkway, Cleveland, OH, USA.
- Holeyman, A.E. and Legrand, C., 1994. Soil modeling for pile vibratory pile driving. Int. Conf. On Design and Construction of Deep Foundations, Vol. 2, pp 116-1178, Orlando, Florida, USA.

Holeyman, A.E., Legrand, C., and Van Rompaey, 1996. A method to predict the driveability of vibratory driven piles, Fifth Int. Conf. On the Use of Stress Wave Measurements on Piles, Orlando, Florida, USA.

Leonards, G.A., Deschamps, R.J., and Feng, Z., 1995. Driveability, load/settlement and bearing capacity of piles installed with vibratory hammers. Final Report submitted to the Deep Foundations Institute. School of Engineering, Purdue University, West Lafayette, Indiana, USA

Likins, G., Rausche, F., Morrison, M., and Raines, R., 1992. Evaluation of measurements for vibratory hammers. 4th Int. Conf. On the Application of Stress Wave Theory to Piles, Balkema, Rotterdam, pp 433 – 436.

Massarsch, K.R., 1992. Static and dynamic soil displacements caused by pile driving. 4th Int. Conf. On the Application of Stress Wave Theory to Piles, Balkema, Rotterdam, pp 15 – 24.

Poulos, H.G. and Davis, E.H., 1980. Pile foundation analysis and design, John Wiley and Sons, Inc.

Rausche, F., Goble, G. G. and Likins, G. 1985. Dynamic determination of pile capacity. Journal of Geotechnical Engineering, ASCE, Vol. 111, No.3, Paper No. 1951:367-383

Smart, J.D., 1969, Vibratory pile driving. Dissertation, Department of Civil Engineering, University of Illinois, USA.

Smith, E.A.L., (1960), "Pile Driving Analysis by the Wave Equation," Journal of the Soil Mechanics and Foundations Division, ASCE, Volume 86.

Viking, K., 2002. Vibro-driveability, a field study of vibratory driven sheet piles in non-cohesive soils, PhD thesis, Div. Of Soil and Rock Mechanics, Royal Inst. Of Technology, Stockholm, Sweden.

White, J., 2002. Super large caissons, lessons learned. Int. Conf. On Vibratory Pile Driving and Deep Soil Compaction, Louvain-la-Neuve, Belgium, Sept. 9-11, Balkema publisher.